Appl. Phys. A (2017) 123:594
DOI 10.1007/s00339-017-1195-8

Applied Physics A
Materials Science & Processing

A widely applicable method to fabricate underwater superoleophobic surfaces with low oil-adhesion on different metals by a femtosecond laser

Jingzhou Zhang[1] · Feng Chen[1] · Qing Yang[2] · Jiale Yong[1] · Jinglan Huo[1] · Yao Fang[1] · Xun Hou[1]

Received: 16 March 2017 / Accepted: 14 August 2017 / Published online: 24 August 2017

Abstract In this paper, a one-step way to realize underwater superoleophobicity and low oil-adhesion on various metals by femtosecond laser ablation was proposed. The laser ablated aluminum surface showed hierarchical rough microstructure composed of abundant micro-holes and nano-particles. The oil contact angle on the as-prepared Al surface reached up to 157° and the oil sliding angle was just 7° to a 1,2-dichloroethane droplet in water. In addition, various oils including chloroform, hexadecane, *n*-dodecane, decane, liquid paraffin, and petroleum ether also showed underwater superoleophobicity on the structured aluminum surface. What's more, other metals such as iron, copper, molybdenum, and stainless steel were ablated, respectively, through the same method. Due to the formation of rough microstructures and their intrinsic high surface energy, they all exhibited remarkable underwater ultralow oil-adhesive superoleophobicity. Such one-fit-all method with anti-oil-pollution can be a suit for an ocean of metals, which undoubtedly will be used in underwater precise instruments, such as vessels, underwater detectors, and oil–water separation device.

✉ Feng Chen
chenfeng@mail.xjtu.edu.cn

✉ Jiale Yong
jlyong@xjtu.edu.cn

1 State Key Laboratory for Manufacturing System Engineering and Key Laboratory of Photonics Technology for Information of Shaanxi Province, School of Electronics and Information Engineering, Xi'an Jiaotong University, Xi'an 710049, People's Republic of China

2 School of Mechanical Engineering, Xi'an Jiaotong University, Xi'an 710049, People's Republic of China

1 Introduction

Liquid wettability of solid surface, which is governed by both the surface chemical composition and the geometrical microstructure of the materials, is an important scientific research field [1–5]. Superoleophobicity, meaning oil contact angle (OCA) greater than 150°, is a special phenomenon of surface wettability [6–8]. In nature, scales of fish and shells of clam can keep themselves clean even in oil-polluted water. In recent years, Jiang's group revealed that these great function properties are caused from their underwater superoleophobicity [9–11]. This special underwater superoleophobicity of them is resulted from the combined action of their hydrophilic chemical components and micro/nanoscale hierarchical rough structures [12].

Metal is widely used in underwater precise instruments such as underwater detectors, underwater robots, and oil–water separating mesh. However, oil contamination in ocean is easy to adhere to these metal surfaces, which usually lower the accuracy of instruments and reduce their service life. Aiming at underwater anti-oil metal research, several underwater superoleophobic surfaces with rough structures have been achieved. Yao et al. reported a high-energy $Cu(OH)_2$ surface with underwater low-adhesive superoleophobicity by wet chemical etching [13]. Wang et al. designed underwater superoleophobic TiO_2 coatings with self-cleaning properties by hydrothermal method [14]. Liu et al. achieved underwater tunable wettability $Cu(OH)_2$ nanoneedle mesh through a chemical oxidation of a smooth-copper mesh [15]. These especial metal surfaces were used in drag reduction, droplet operation, microfluidic, oil/water separation, and many other fields [13, 15–20]. However, the above-mentioned methods to build micro/nanoscale rough structures are just limited to specific kind of metals. A one-fit-all and effective method that can directly achieve underwater superoleophobicity on various metals has yet to be explored.

As a new processing technology, femtosecond laser microfabrication has been recently used to fabricate micro/nanohierarchical rough structures to control the wettability of solid surfaces [21–25]. Compared to the traditional technology, femtosecond laser ablation has the ability to one-step form multi-scale rough structures with high accuracy [26–29]. Meanwhile, building multi-scale rough surfaces does not rely on chemical reactions, so that this method can be applied to a great number of materials including those difficult to be set off a chemical reaction [30].

Here, we report a widely applicable method to achieve underwater superoleophobic surfaces with low oil-adhesion on different metals such as aluminum, iron, copper, molybdenum, and stainless steel by femtosecond laser ablation. After being treated by a femtosecond laser ablating process, multifarious metal surfaces presented a consistent high roughness. Controlled the average distance (AD) of laser pulse-ablated point from 2 to 20 μm, all those surfaces showed underwater superoleophobicity (OCA >150°) for various oil droplets, such as 1,2-dichloroethane, chloroform, hexadecane, *n*-dodecane, decane, and petroleum ether. Meanwhile, oil droplets could roll down easily only if the laser-induced rough metal surface had a small-angle inclination.

2 Experimental section

Aluminum plate with thickness of 0.3 mm was first scanned by femtosecond laser in air environment. The ablating process was introduced in our previous work [31]. The sample was mounted on a three-dimensional machining stage controlled by computer program and then ablated by a regenerative amplified Ti: sapphire laser system (CoHerent, Libra-usp 1 K-he-200) with pulse duration of 50 fs, center wavelength of 800 nm, and repetition of 1 kHz. The laser beam with energy of 10 mw was focused by a microscope objective lens (NA = 0.45, 20× Nikon) on the sample surface. We controlled the AD by changing scanning speed and the interval of lines during the line-by-line femtosecond laser ablating process, as shown in Fig. 1. For example, the structured sample with AD = 2 μm can be achieved at the scan speed of 2 mm/s and scanning line interval of 2 μm. After that, the sample was cleaned in acetone, alcohol, and deionized water by ultrasonic cleaner one after another.

The microstructure of the sample was observed by a Quanta F250 scanning electron microscope (SEM, FEI, America) and JSM-6390A SEM (JEOL, Japan). The roughness and cross-sectional profiles of the surfaces were investigated by a LEXT-OLS4000 laser confocal microscope (Olympus, Japan). A JC2000D contact-angle system (POWEREACH, China) was used to measure the contact angles (CAs) and the sliding angles (SAs) of 8 μL microdroplets of oil and water on the as-prepared surfaces, respectively. Particularly, for the underwater OCA and oil sliding angle (OSA) measurements, the sample was mounted on a transparent sink full of pure water instead of being placed on the sample stage directly. For oil selection, 1,2-dichloroethane was chosen as representative heavy oil, while chloroform, hexadecane, *n*-dodecane, decane, and petroleum ether were tested as supplements. All the mean values of OCA and OSA were obtained by measuring at three different places on the same sample. Following the same procedure, rough microstructures as well as underwater superoleophobicity were also formed on femtosecond laser-ablated iron, copper, molybdenum, and stainless steel surfaces.

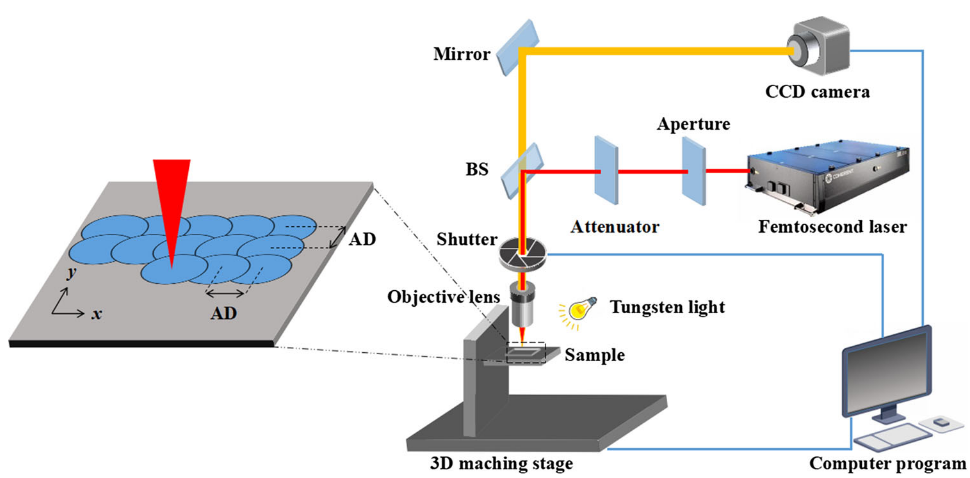

Fig. 1 Schematic illustration of the experimental setup and the fabrication process

3 Results and discussion

3.1 Morphology features

Figure 2 shows the SEM images of unprocessed aluminum surface (Fig. 2a) and the femtosecond laser ablated aluminum surface with the AD = 2 μm (Fig. 2b–d). There are many micro-holes uniformly arranging based on a square-shaped array with the period of 10 μm. Further magnified SEM image reveals that the domain above the micro-holes is characterized by a great number of irregular nano-particles. The average diameter and depth of the holes are about 7 and 4.1 μm (Fig. 2e). The micro-protrusions and the nano-particles increase the roughness (R_a) from 0.102 to 1.227 μm. This micro/nanoscale structure dramatically increases the real contact area between water and aluminum surface, so that it contributes to amplify the wettability of aluminum surface.

3.2 Wettability

As shown in Fig. 3a, like the vast majority of metal, aluminum had intrinsic hydrophilicity in air. After femtosecond laser irradiation, the water contact angle (WCA) decreased from 84.7 ± 1° to 28.1 ± 0.6° (Fig. 3b). Micro/nano hierarchical rough structures enhanced the hydrophilicity of aluminum. In water, an oil droplet on an unprocessed aluminum surface retained a nearly spherical shape (Fig. 3c). Flat aluminum showed ordinary oleophobicity with OCA = 138.5 ± 1°. However, when an oil droplet was placed on the as-prepared aluminum surface in water, the shape of oil droplet was like a sphere and the OCA increased to 157 ± 0.5° (Fig. 3d). Hence, the as-prepared surface was endowed with underwater superoleophobicity by the femtosecond laser microfabrication.

The underwater oil-adhesion of the irradiated surface can be directly reflected by measuring OSA. In this test, an

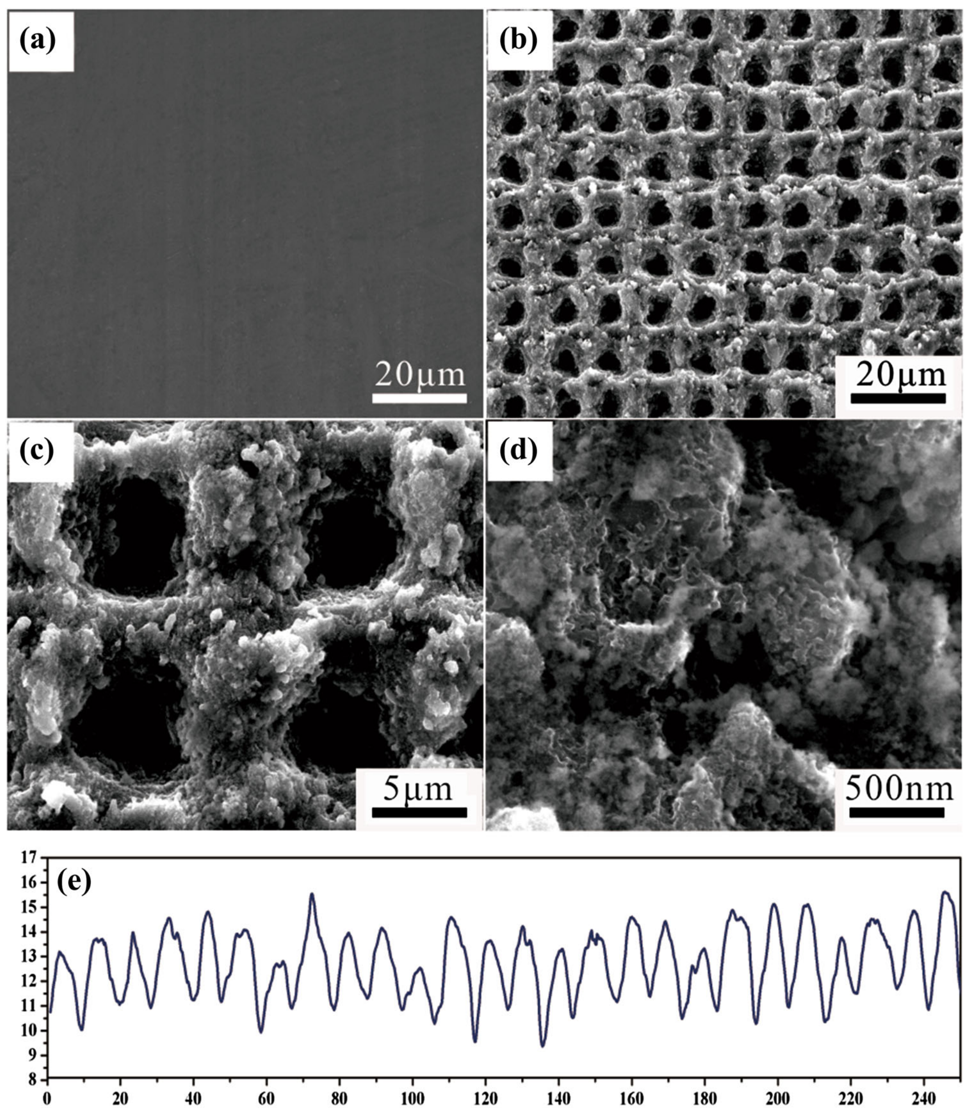

Fig. 2 SEM images of the aluminum before (**a**) and after being ablated by a femtosecond laser with different magnification: **b** ×3000, **c** ×12,000, **d** ×100,000. **e** Cross-sectional profiles of the as-prepared surface

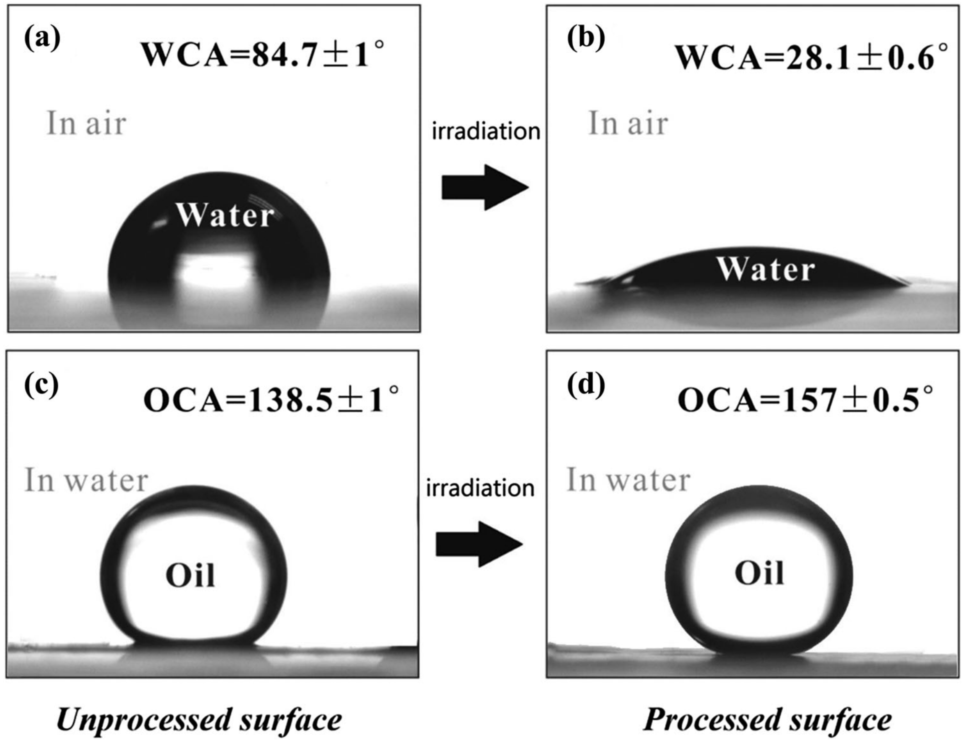

Fig. 3 An 8 μL water droplet on: **a** the unprocessed aluminum sample and **b** the processed aluminum sample in air. 8 μL oil droplet on: **c** the unprocessed aluminum sample and **d** the processed aluminum sample in water

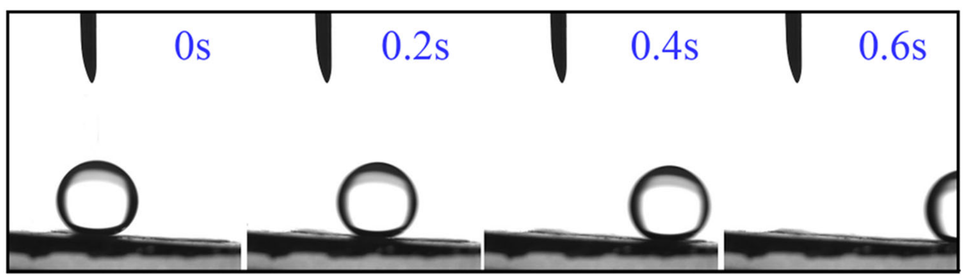

Fig. 4 Time sequence of snapshots of an 8 μL oil droplet rolling on the 4° tilted sample

8 μL oil droplet was placed on the irradiated rough aluminum surface in water and then the sample was tilted slowly. As soon as the tilt angle was increased to 4°, the oil droplet began to roll down. Figure 4 shows the time sequence of snapshots of the oil droplet rolling down on the tilted sample. The OSA of 4° was so small that an oil microdroplet could roll down just by slight tilting or shaking. Therefore, the laser-induced rough aluminum surface exhibited not only superoleophobicity but also ultralow oil-adhesion in water.

3.3 Time evolution of the underwater superoleophobicity

Stability of time evolution is important in wettability flied [32, 33]. Figure 5 shows the OCA values of underwater oil droplets on the laser-ablated aluminum surfaces stored in water for different time. The OCA decreases from 157° to 152° as storage time changes from 1 to 12 h. And then it becomes stable. It can be seen that the OCAs are always larger than 150° over time, showing the favorable stability of the rough aluminum surfaces.

3.4 Universality of the femtosecond laser microfabrication

Femtosecond laser fabrication can build up rough microstructures with different AD on aluminum (Fig. 6a–c). As the AD increases from 2 to 20 μm, the R_a gradually decreases from 1.227 to 0.187 μm (Fig. 6d). Figure 6e depicts the OCA and OSA values of an underwater oil droplet on the laser ablated aluminum surfaces with different AD. It can be seen that the OCAs are stable at 157 ± 1° and the OSAs are always less than 4° as AD increased from 2 to 20 μm. Obviously, all the OCAs are higher than 150° and all the OSAs are lower than 10°, meaning that the underwater superoleophobic surfaces with low oil-adhesion can be realized in a wide technology

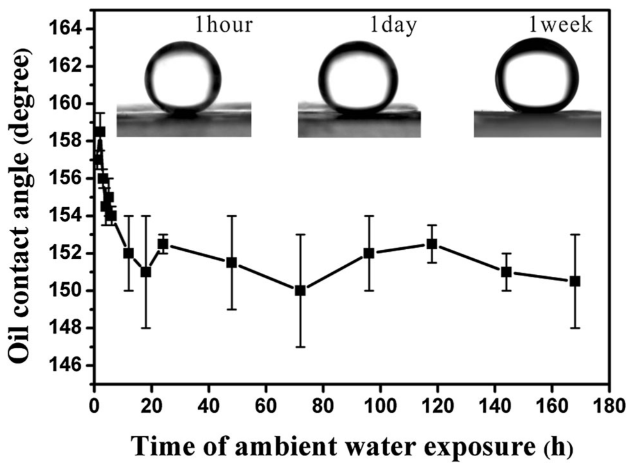

Fig. 5 Plot of as-prepared aluminum OCA as a function of ambient water exposure time. Oil droplets staying on the samples which store in water for different times are shown in the *insets images*, respectively

parameter range of AD. Hence, forming micro/nanoscale hierarchical rough structures by a femtosecond laser to achieve superoleophobicity is a feasible and practical method in wide ranges.

In addition, the femtosecond laser ablated rough aluminum plate (AD = 2 μm) also presents underwater superoleophobicity and ultralow oil-adhesion to various oils with different surface tensions, such as chloroform, hexadecane, *n*-dodecane, decane, liquid paraffin, and petroleum ether. As shown in Fig. 7, those oil droplets on the as-prepared surface have the OCAs all larger than 150° and can easily roll down as soon as the surface is tilted at very small angle (<1°).

Moreover, femtosecond laser ablation can also endow other different types of industrial metals, such as copper, iron, molybdenum, and stainless steel, with underwater superoleophobicity by the same one-step scanning method. Figure 8 shows the SEM images of different metal surfaces after laser irradiation at AD = 2 μm. Left column of images shows the high roughness of copper (Fig. 8a), iron (Fig. 8c), molybdenum (Fig. 8e), and stainless steel (Fig. 8g), while higher magnifications of the microstructures are on the right column, respectively. After laser irradiation, each sample exhibits particular nanoscale rough structures and the surface roughness (R_a) is about 1.14, 0.41, 0.49, and 0.42 μm, respectively. Although these nanoscale structures (Fig. 8b, d, f, h) differ from the

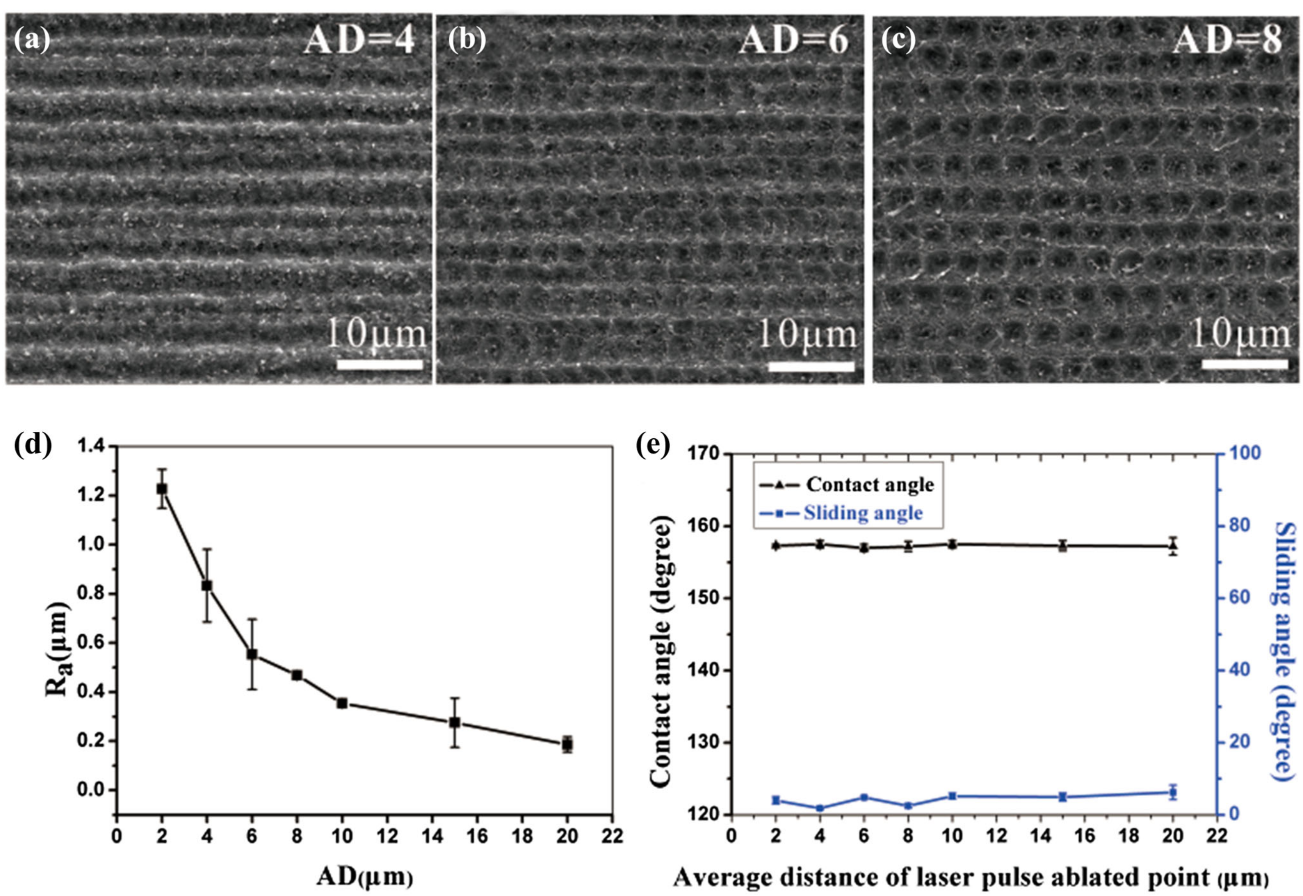

Fig. 6 SEM images of the aluminum surfaces after femtosecond irradiation: **a** AD = 4 μm; **b** AD = 6 μm; **c** AD = 8 μm. **d** Relationship between R_a and the AD. **e** Relationships between the underwater OCA (*left*)/OSA (*right*) values and the AD

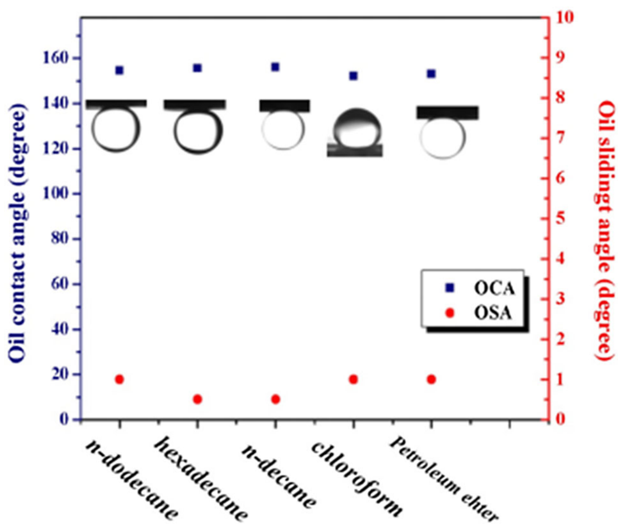

Fig. 7 Underwater superoleophobicity and ultralow oil-adhesion of various oils on the femtosecond laser ablated rough aluminum surface

aluminum samples on which it bestrews micro-holes and nano-particles, such irregular nano-particles also provide enough roughness to enlarge the real contact area between solid and water. The laser-induced rough nanostructures result in underwater low oil-adhesive superoleophobicity on the copper, iron, molybdenum, and stainless steel surfaces. As shown in the insets of Fig. 8, all the oil droplets placed on the as-prepared metal surfaces in water are nearly spherical and OCAs are 157 ± 1°, 155 ± 0.5°, 152 ± 0.5°, 155.5 ± 0.5°, respectively. Oil droplet can be easily rolled down by microvibration. It demonstrates that this simple way to achieve underwater superoleophobicity fits for not only aluminum but also a wide range of other metals.

This method avoids the material limitation of other traditional approach and is a one-fit-all way to generate underwater superoleophobicity on various metals surfaces.

3.5 Theoretical explanation

Since most of the metals and their metallic oxides have high surface free energy and show hydrophilic properties in air (Fig. 9a), we just need to build rough microstructures to realize underwater superoleophobicity on metals surface. Here, the micro/nano structures play a key role in forming superoleophobic metal surfaces in water [6, 34–41]. After femtosecond laser irradiation, the flat metal surface changes into high roughness with superhydrophilicity in air, and the surface is in Wenzel's state, as shown in Fig. 9b. And the WCA can be expressed by Wenzel's equation [9]:

$$\cos\theta_r = k \cdot \cos\theta \qquad (1)$$

where θ_r and θ are the WCA on rough surface and ideal flat surface in air environment, respectively. The roughness factor k is the ratio between the real contact area and projected area, which is always large than 1. For metal, ideal contact angle θ is smaller than 90°, so $\cos\theta_r > \cos\theta$, revealing $\theta_r < \theta < 90°$. It means that rough microstructures enhance the hydrophilicity of original hydrophilic material. According to Eq. (1), the value of k of the as-prepared aluminum surface (AD = 2 μm) can be inferred to be 10.1 ($\theta_r = 28°$ and $\theta = 85°$), which indicates that the water contact area is strongly increased.

As it was reported previously, oil microdroplet is hard to come into contact with the hydrophilic surfaces in water environment, where water layer is already trapped tightly by hydrophilic materials. Therefore, hydrophilic surfaces exhibit underwater oleophobic property (Fig. 9a, c). The more hydrophilic the surface is, the more underwater oleophobic the surface is. After femtosecond laser irradiation, formed structures help metal surface trap water tightly and an underwater Cassie state formed in the water–oil–solid system. As shown in Fig. 9d, these rough solid surfaces trap water molecules easier than oil molecules, so that the real contact area between oil and metal surface is parlously decreased by water layer [40]. Hence, it leads to the jointly large OCA and small OSA underwater. According to underwater Cassie's equation [8, 42]:

$$\cos\theta'_{ow} = f \cdot \cos\theta_{ow} + f - 1 \qquad (2)$$

where θ_{ow} and θ'_{ow} are the OCA of an oil droplet on the unprocessed (flat) and processed (rough) sample, respectively. The factor f is the oil projected wet area, which is negatively related to roughness in water. Cassie's equation reveals that the θ'_{ow} increases as the f decreases, when θ_{ow} is larger than 90°. The underwater Cassie's state proves that the rough microstructures achieved by femtosecond laser are able to endow metal with the underwater superoleophobic property ($\theta'_{ow} > 150°$). According to Eq. (2), the value of f of the as-prepared aluminum surface (AD = 2 μm) can be inferred to be 0.32 ($\theta_{ow} = 138°$ and $\theta'_{ow} = 157°$), which indicates that the trapped water layer in rough microstructures greatly decreased the real contact area between oil droplet and metal surface, resulting in very low oil-adhesion underwater [40, 43, 44].

4 Conclusions

In conclusion, underwater superoleophobicity with ultralow oil-adhesion was achieved on different metal surfaces by femtosecond laser microfabrication. The OCAs of a 1,2-dichloroethane droplet were always larger than 150°, while the oil droplets could easily roll down on the laser ablated aluminum surfaces with the AD ranging from 2 to 20 μm. Such underwater superoleophobicity and ultralow oil-

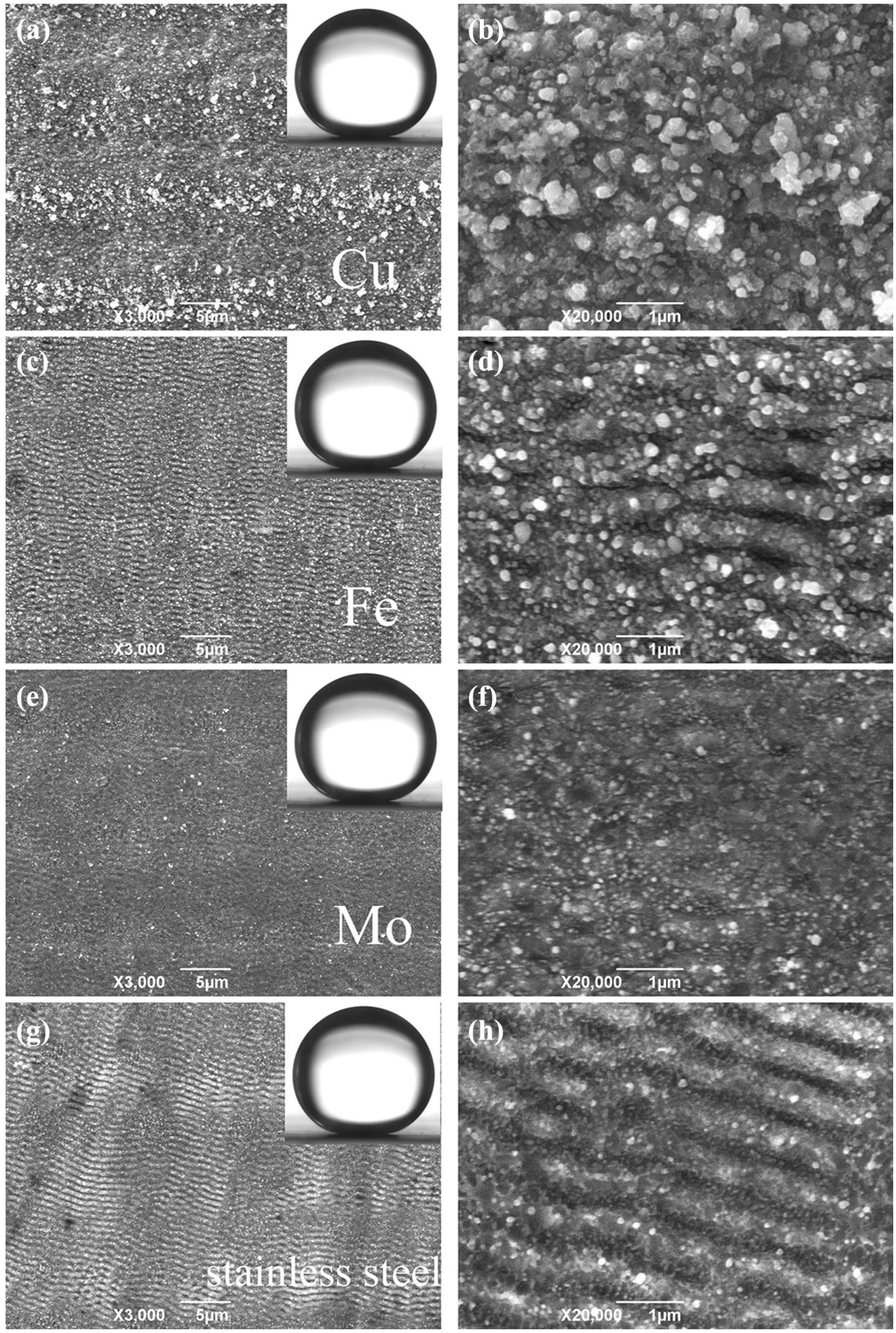

Fig. 8 SEM images of the femtosecond laser-induced rough microstructures on various metal substrates with AD = 2 μm: **a**, **b** copper, **c**, **d** iron, **e**, **f** molybdenum, and **g**, **h** stainless steel. Oil droplets staying on the samples are shown in the *insets of left column images*, respectively

adhesion were also verified by other different types of oil droplets including chloroform, hexadecane, *n*-dodecane, decane, liquid paraffin, and petroleum ether. Furthermore, after femtosecond laser irradiation, other metals such as iron, copper, molybdenum, and stainless steel also showed remarkable underwater superoleophobicity. The femtosecond laser ablating process is a widely applicable method to fabricate underwater superoleophobic metal surfaces. Their similar low oil-adhesions and superoleophobic properties resulted from their high roughness of microstructures. In water, the structures trap water molecules easier than oil molecules, so that the real contact area between oil and metal surface is strongly decreased. This useful method can endow an ocean of metals with underwater

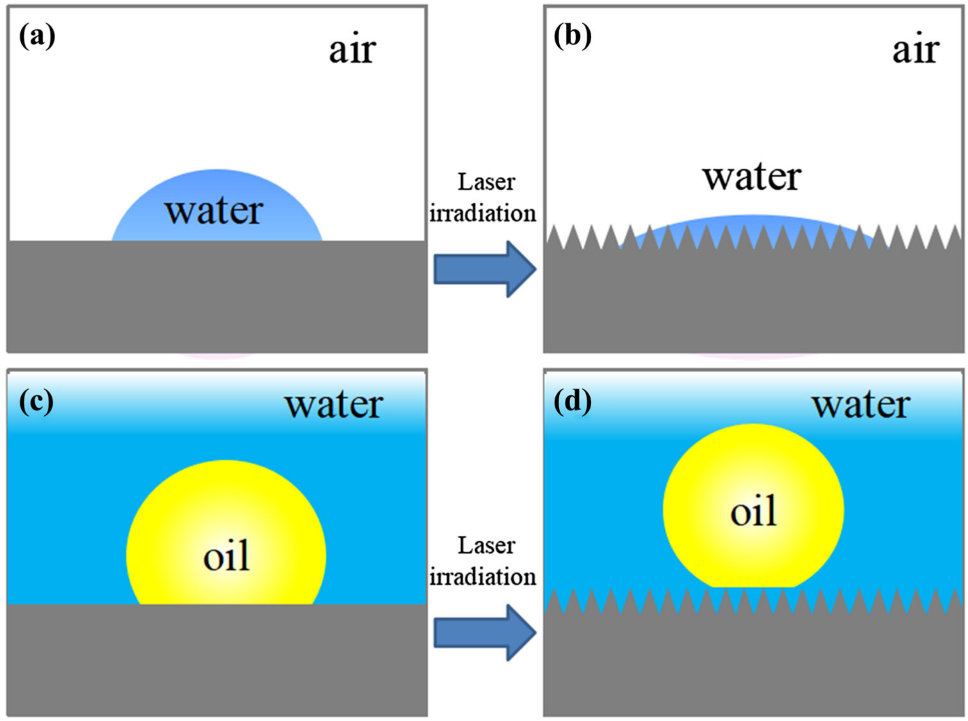

Fig. 9 Schematic diagram of the formation of underwater superoleophobic metal surface irradiated by femtosecond laser. **a** Water droplet on flat hydrophilic surface in air. **b** Water droplet on a laser-induced rough metal surface in air. **c** Oil droplet on a flat hydrophilic surface in water. **d** Oil droplet on a laser-induced rough metal surface in water

superoleophobicity, which undoubtedly will be used in our future life with bright prospect, such as drag reduction, droplet operation, microfluidic, oil/water separation, just to name only a few.

Acknowledgements This work is supported by the National Science Foundation of China under the Grant nos. 51335008 and 61475124, the NSAF Grant no. U1630111, the Special-funded programme on national key scientific instruments and equipment development of China under the Grant no. 2012YQ12004706, the National Key Research and Development Program of China under the Grant no. 2017YFB1104700, China Postdoctoral Science Foundation under the Grant no. 2016M600786, and the Collaborative Innovation Center of Suzhou Nano Science and Technology and the International Joint Research Center for Micro/Nano Manufacturing and Measurement Technologies.

References

1. F. Xia, L. Jiang, Adv. Mater. **20**, 2842–2858 (2008)
2. Y.L. Zhang, H. Xia, E. Kim, H.B. Sun, Soft Matter **8**, 11217–11231 (2012)
3. J. Genzer, K. Efimenko, Biofouling **22**, 339–360 (2006)
4. J.L. Yong, F. Chen, Q. Yang, Y. Fang, J.L. Huo, X. Hou, Chem. Commun. **51**, 9813–9816 (2015)
5. X. Yao, Y.L. Song, L. Jiang, Adv. Mater. **23**, 719–734 (2011)
6. J.L. Yong, F. Chen, Q. Yang, G.Q. Du, C. Shan, H. Bian, U. Farooq, X. Hou, J. Mater. Chem. A **3**, 9379–9384 (2015)
7. J.L. Yong, F. Chen, Q. Yang, J. Huo, X. Hou, Chem. Soc. Rev. **46**, 4168–4217 (2017)
8. D. Wu, S.Z. Wu, Q.D. Chen, S. Zhao, H. Zhang, J. Jiao, J.A. Piersol, J.N. Wang, H.B. Sun, L. Jiang, Lab Chip **11**, 3873–3879 (2011)
9. M.J. Liu, S.T. Wang, Z.X. Wei, Y.L. Song, L. Jiang, Adv. Mater. **21**, 665–669 (2009)
10. X.L. Liu, J. Zhou, Z.X. Xue, J. Gao, J.X. Meng, S.T. Wang, L. Jiang, Adv. Mater. **24**, 3401–3405 (2012)
11. Y. Cai, L. Lin, Z.X. Xue, M.J. Liu, S.T. Wang, L. Jiang, Adv. Funct. Mater. **24**, 809–816 (2014)
12. L. Lin, M.J. Li, L. Chen, P.P. Chen, J. Ma, D. Han, L. Jiang, Adv. Mater. **22**, 8426–8430 (2010)
13. X. Yao, J. Gao, Y.L. Song, L. Jiang, Adv. Funct. Mater. **21**, 4270–4276 (2011)
14. H. Wang, Z.G. Guo, Appl. Phys. Lett. **104**, 183703 (2014)
15. J. Liu, L. Wang, N. Wang, F. Guo, L. Hou, Y. Chen, J. Liu, Y. Zhao, L. Jiang, Small **13**, 1600499 (2017)
16. X.L. Liu, J. Gao, Z.X. Xue, L. Chen, L. Lin, L. Jiang, S.T. Wang, ACS Nano. **6**, 5614–5620 (2012)
17. C.M. Ding, Y. Zhu, M.J. Liu, L. Feng, M.X. Wan, L. Jiang, Soft Matter **8**, 9064–9068 (2012)
18. Y. Sawai, S. Nishimoto, Y. Kameshima, E. Fujii, M. Miyake, Langmuir **29**, 6784–6789 (2013)
19. C.F. Wang, F.S. Tzeng, H.G. Chen, C.J. Chang, Langmuir **28**, 10015–10019 (2012)
20. Q. Wen, J.C. Di, L. Jiang, J.H. Yu, R.R. Xu, Chem. Sci. **4**, 591–595 (2013)
21. V. Zorba, E. Stratakis, M. Barberoglou, E. Spanakis, P. Tzanetakis, S.H. Anastasiadis, C. Fotakis, Adv. Mater. **20**, 4049–4054 (2008)
22. J.L. Yong, Q. Yang, F. Chen, D.S. Zhang, U. Farooq, G.Q. Du, X. Hou, J. Mater. Chem. A **2**, 5499–5507 (2014)
23. J.L. Yong, F. Chen, Q. Yang, D.S. Zhang, U. Farooq, G.Q. Du, X. Hou, J. Mater. Chem. A **2**, 8790–8795 (2014)
24. J.L. Yong, Q. Yang, F. Chen, H. Bian, G.Q. Du, U. Farooq, X. Hou, Adv. Mater. Interfaces **2**, 1400388 (2015)
25. J.L. Yong, F. Chen, Q. Yang, U. Farooq, H. Bian, G.Q. Du, X. Hou, Appl. Phys. Lett. **105**, 071608 (2014)
26. D.J. Hwang, T.Y. Choi, C.P. Grigoropoulos, Appl. Phys. A **79**, 605–612 (2004)

27. J. Bonse, K.-W. Brzezinka, A.J. Meixner, Appl. Surf. Sci. **221**, 215–230 (2004)
28. M.Y. Shen, C.H. Crouch, J.E. Carey, E. Mazur, Appl. Phys. Lett. **85**, 5694–5696 (2004)
29. J.L. Yong, F. Chen, Q. Yang, Y. Fang, J. Huo, J. Zhang, X. Hou, Adv. Mater. Interfaces (2017). doi:10.1002/admi.201700552
30. J. Bonse, S. Baudach, J. Kriiger, W. Kautek, M. Lenzner, Appl. Phys. A **74**, 19–25 (2002)
31. J.L. Yong, F. Chen, Q. Yang, D.S. Zhang, H. Bian, G.Q. Du, J.H. Si, X.W. Meng, X. Hou, Langmuir **29**, 3274–3279 (2013)
32. A.I. Aria, P.R. Kidambi, R.S. Weatherup, L. Xiao, J.A. Williams, S. Hofmann, J. Phys. Chem. C **120**, 2215–2224 (2016)
33. J. Winter, S. Rapp, M. Schmidt, H.P. Huber, Appl. Surf. Sci. **414**, 313–324 (2017)
34. Q. Zhu, Q.M. Pan, F.T. Liu, J. Phys. Chem. C **115**, 17464–17470 (2011)
35. M.H. Jin, S.S. Li, J. Wang, Z.X. Xue, M.Y. Liao, S.T. Wang, Chem. Commun. **48**, 11745–11747 (2012)
36. Z.X. Xue, S.T. Wang, L. Lin, L. Chen, M.J. Liu, L. Feng, L. Jiang, Adv. Mater. **23**, 4270–4273 (2011)
37. M.J. Liu, X.L. Liu, C.M. Ding, Z.X. Wei, Y. Zhu, L. Jiang, Soft Matter **7**, 4163–4165 (2011)
38. U. Manna, D.M. Lynn, Adv. Funct. Mater. **25**, 1672–1681 (2015)
39. T. Yuan, J.Q. Meng, T.Y. Hao, Z.H. Wang, Y.F. Zhang, ACS Appl. Mater. Interfaces **7**, 14896–14904 (2015)
40. J.L. Yong, F. Chen, Q. Yang, H. Bian, G.Q. Du, C. Shan, J.L. Huo, Y. Fang, X. Hou, Adv. Mater. Interfaces **3**, 1500650 (2016)
41. S. Wang, L. Jiang, Adv. Mater. **19**, 3423–3424 (2007)
42. Z.J. Cheng, H. Lai, Y. Du, K.W. Fu, R. Hou, N.Q. Zhang, K.N. Sun, ACS Appl. Mater. Interfaces **5**, 11363–11370 (2013)
43. L. Chen, M.J. Liu, H. Bai, P.P. Chen, F. Xia, D. Han, L. Jiang, J. Am. Chem. Soc. **131**, 10467–10472 (2009)
44. Q.F. Cheng, M.Z. Li, Y.M. Zheng, B. Su, S.T. Wang, L. Jiang, Soft Matter **7**, 5948–5951 (2011)